Structural Phase Transitions of Vortex Matter in an Optical Lattice

H. Pu,[1] L. O. Baksmaty,[2] S. Yi,[1] and N. P. Bigelow[2]

[1]*Department of Physics and Astronomy, and Rice Quantum Institute, Rice University, Houston, Texas 77251-1892, USA*

[2]*Department of Physics and Astronomy, and Laboratory for Laser Energetics, University of Rochester, Rochester, New York 14627, USA*

(Received 28 April 2004; published 16 May 2005)

We consider the vortex structure of a rapidly rotating trapped atomic Bose-Einstein condensate in the presence of a corotating periodic optical lattice potential. We observe a rich variety of structural phases which reflect the interplay of the vortex-vortex and vortex-lattice interactions. The lattice structure is very sensitive to the ratio of vortices to pinning sites and we observe structural phase transitions and domain formation as this ratio is varied.

DOI: 10.1103/PhysRevLett.94.190401 PACS numbers: 03.75.Mn, 03.75.Nt

Structural phase transitions occur in a wide range of systems [1]. Studies of structural phase transitions are both of technological importance and of fundamental interest. Technologically, an understanding of structural phase transitions is essential to the study of many materials, while fundamentally they are related to a variety of questions in statistical mechanics, crystallography, magnetism, and surface science, to name a few. Among the most intensively studied systems related to structural phase transitions are graphite intercalation compounds, niobates, adsorbed molecular monolayers and vortex matter in type-II superconductors. In this Letter, we introduce a new system of study, that of vortex matter created in a trapped Bose-Einstein condensate (BEC) formed in the presence of a corotating optical lattice (OL). This system has the advantage of being experimentally realizable, tunable over a wide range of interaction parameters, and describable by an *ab initio* theory.

We take inspiration from two recent developments in atomic BECs. The first is the observation of vortex-lattice excitations in rapidly rotating BECs [2]. The second is the set of proposals and demonstrations concerning periodic optical lattice potentials created using holographic phase plates [3] or amplitude masks [4]. This latter technique means that a rotating OL (at a desired angular frequency) can be realized by simply rotating the OL phase plate or mask. The amenability of BECs to imaging, experimental control, and theoretical description makes the atomic condensate an attractive test bed for many phenomena frequently encountered but often difficult to study in other systems. One such example is given by the recent spectacular realization of the superfluid-Mott insulator quantum phase transition in a condensate confined by an optical lattice [5] following a proposal of Jaksch *et al.* [6]. This transition was theoretically predicted over a decade ago [7] in the context of liquid ^{4}He absorbed in porous media but has eluded direct observation.

In our system, the phase transition is observed as a shift in geometry of the vortex lattice as optical parameters are tuned. This situation is analogous to that of type-II superconductors subject to external magnetic field and artificial periodic pinning [8–10]. In the analogy, the angular rotation $\Omega\hat{z}$ of the BEC and the peaks of the OL play the role of the magnetic field and the pinning centers, respectively. In contrast to the pinning lattice in typical superconducting samples, the periodicity and depth of the optical lattice may be dynamically tuned in an atomic system. Furthermore, the clean microscopic physics of atomic BECs makes a first-principles calculation possible based on a mean-field treatment. This is in contrast to the superconductor case, where theoretical calculations frequently rely on elegant but phenomenological models or on molecular dynamics simulations [9].

We work in a pancake shaped geometry. For the BEC, this is justified because at high rotation rates, the centrifugal forces reduce the radial trapping frequency $\omega_\perp$, and the condensate may be accurately assumed to be frozen into the harmonic oscillator ground state in the axial direction ($\hat{z}$). We therefore integrate the axial degree of freedom, obtaining an effective two-dimensional system with a renormalized coupling constant. In a frame rotating with angular velocity $\Omega\hat{z}$, the transverse wave function $\phi(x, y)$ obeys the two-dimensional time-dependent Gross-Pitaevskii equation:

$$i\frac{\partial\phi}{\partial t} = \left[-\frac{1}{2}\nabla^2 + \frac{r^2}{2} + V_{\rm lat} + U|\phi|^2 - \mu - \Omega L_z\right]\phi. \quad (1)$$

Unless otherwise specified we choose our units for time, length, and energy as $1/\omega_\perp$, $\sqrt{\hbar/(m\omega_\perp)}$, and $\hbar\omega_\perp$, respectively. Here $r^2 = x^2 + y^2$, U is the (renormalized) effective 2D nonlinear interaction coefficient, μ the chemical potential, L_z the z component of the angular momentum operator, and $V_{\rm lat} = V_0[\sin^2(kx) + \sin^2(ky)]$ the optical lattice potential. In this work, we consider only the case where the optical lattice is corotating with the condensate; thus $V_{\rm lat}$ in Eq. (1) is time independent.

For each chosen value of the OL periodicity (denoted by $a = \pi/k$), we vary the peak-to-peak potential amplitude of the optical lattice V_0 from 0 to $V_{\rm max}$, the value at which the lattice is fully pinned. We obtain the ground state of the system for a given set of parameters (V_0, a, Ω) by prop-

agating Eq. (1) in imaginary time (i.e., by steepest descent). To ensure that the obtained structure corresponds to the ground state, we usually start with several different initial trial wave functions possessing different symmetries. We include trial vortex lattices with both regular structures (triangular, square, etc.) and irregular shape. In our calculation, we use the ^{87}Rb parameters of the JILA experiment [2]: $\omega_\perp = 2\pi \times 8.3$ Hz, $\omega_z = 2\pi \times 5.3$ Hz, $\Omega = 0.95\omega_\perp$, and the total particle number is taken to be 2×10^5. One may be concerned that for a faster rotating speed the vortex core size will increase and eventually become larger than the intervortex spacing. This, however, turns out not to be true. As predicted by Fischer and Baym [11], and experimentally confirmed in Ref. [2], the core size remains a limiting fraction of the intervortex spacing even as $\Omega \rightarrow \omega_\perp$.

Evidently, both the atomic and the optical parameters affect the ground state. For simplicity, in this work we focus on the effect resulting from variation of the OL. Our variables are therefore the depth (V_0) and periodicity (a) of the optical potential. Specifically, a defines the density of pinning sites which occur at the peaks of the OL potential, whereas Ω determines the density of vortices. As found in previous studies [9], we observe that the structure of the fully pinned vortex lattice is very sensitive to the ratio η defined as $\eta = N_v/N_p$, where N_v and N_p are the density of vortices and pinning sites, respectively. For the OL potential we use here, $N_p = 1/a^2$. In the absence of the OL, $N_v = 2/(\sqrt{3}\epsilon^2)$, where $\epsilon = [2\pi/(\sqrt{3}\Omega)]^{1/2}$ is the intervortex spacing in a completely unpinned ($V_0 = 0$) vortex lattice [12]. This value of N_v is not significantly changed by the presence of the OL. Hence we take $\eta \approx 2a^2/(\sqrt{3}\epsilon^2)$. In brief, we find that when $\eta \approx 1/2$ the fully pinned vortex lattice has a checkerboard structure and that when $\eta \approx 1$ we obtain a square lattice, while when $\eta \approx 2$ we obtain a square lattice of doubly charged vortices. We remark that, although these results are similar to those obtained in the study of superconductors, this case is by no means obviously *a priori*. This is because the superconductor system is essentially homogeneous and possesses a healing length orders of magnitude smaller than the intervortex spacing, while the atomic system has a finite size due to the confining harmonic potential and the condensate healing length is typically a significant fraction of the intervortex spacing. As a result, the intervortex interaction in the former case can be accurately modeled by a two-body logarithmic repulsive potential, while that in the latter may have a many-body character [13]. In fact, it is possible in the atomic system to tune the parameters from the two-body to the many-body regime and investigate the physical behaviors in different regimes.

The trends in our results are graphically illustrated in Fig. 1, our main result. For three values of a the ground state vortex structure is plotted for increasing values of V_0. The upper, middle, and lower rows correspond to different pinning site densities represented by $\eta = 2$, 1.15, and 0.5, respectively. In the absence of the OL, the angular momentum of the condensate is carried in singly quantized vortices which organize into a triangular Abrikosov lattice. Such vortex lattices have been observed [14], perturbed [2], and accurately described [15] by several groups in recent years.

Not surprisingly, for sufficiently small V_0 the vortex lattice maintains a triangular geometry with only slight distortions (see first column of Fig. 1). In the opposite extreme, at sufficiently large values of V_0, all the vortices are pinned to the antinodes of the OL potential, mirroring the geometry set by the OL potential. What is remarkable are the states that exist between these extremes. At $a = 4\epsilon/3$ (upper row of Fig. 1), there are about twice as many vortices as pinning sites ($\eta \approx 2$), and the fully pinned vortex lattice is found to be a square lattice of doubly quantized vortices which is commensurate with the OL, a

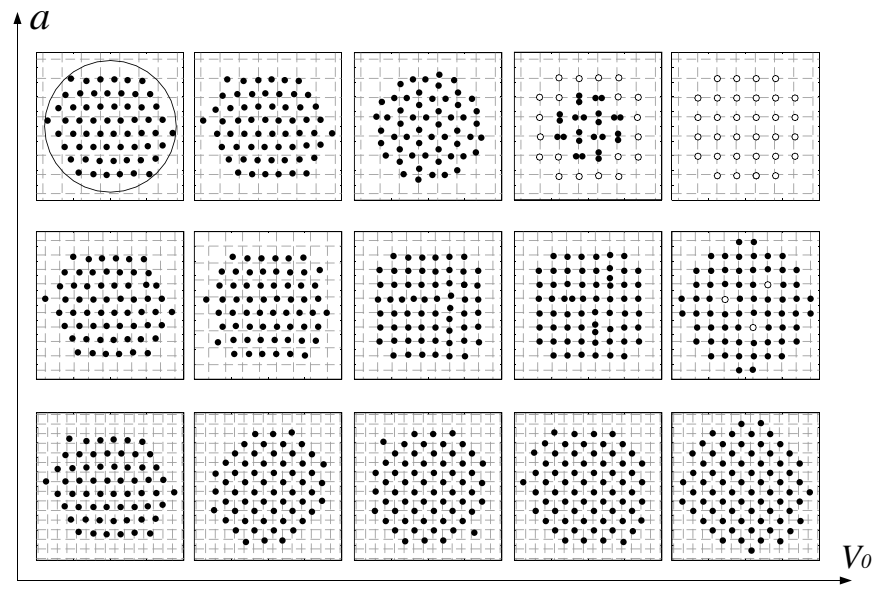

FIG. 1. Structure of the ground state. Each intersection of the dashed lines represents an antinode of the optical potential. Solid (●) and open (○) circles represent the positions of singly and doubly quantized vortices, respectively. Only the positions of vortices within the Thomas-Fermi radius are shown. The Thomas-Fermi boundary $R_{\mathrm{TF}} = \sqrt{2\mu}$ is represented by the circle in the upper-left plot. The upper, middle, and lower rows correspond to $a = 4\epsilon/3$, ϵ, and $2\epsilon/3$, or $\eta \approx 2$, 1.15, and $1/2$, respectively. From left to right, $V_0 = 0.05$, 0.2, 0.5, 2.0, and 5.0, respectively.

situation analogous to the second matching field case for the superconductor system in which the observation of a square double-quanta vortex lattice was reported in Ref. [10]. At a higher pinning site density defined by $a = \epsilon$ (middle row of Fig. 1, $\eta \approx 1.15$), most of the antinodes of the OL are occupied by singly quantized vortices, with the exception of three doubly quantized vortices. And finally, at $a = 2\epsilon/3$ (lower row of Fig. 1, $\eta \approx 1/2$), every next-nearest-neighbor site of the OL is occupied by a singly quantized vortex, and the fully pinned vortex lattice forms what can be described as a ''checkerboard'' square lattice rotated 45° with respect to the OL, once again analogous to the half matching field case of the superconductor system [9].

For intermediate values of V_0, the vortices form structures in between the triangular lattice and the fully pinned vortex lattice, the details of which also depend on the period of the OL. For example, at $a = 4\epsilon/3$, for which the fully pinned vortex lattice is a square lattice of doubly charged vortices, we observe bound pairs centered around the OL pinning sites for the potential depth in the range $0.5 < V_0 < 4.0$. We point out that the orientation of each pair is orthogonal to all adjacent ones. As V_0 increases, these pairs are more and more tightly bound and eventually all pairs collapse onto the corresponding pinning sites, thus forming doubly quantized vortices. Further increasing the OL period, vortices with higher and higher winding number will start to appear in the fully pinned vortex lattice. A single doubly charged vortex was recently observed in atomic condensate and was found to be dynamically unstable [16]. We hope our study here may stimulate more experimental work on multiply charged vortices.

In order to characterize the structural phase transition more quantitatively, we calculate the structure factor [9] of the vortex lattice defined as

$$S(\mathbf{k}) = \frac{1}{N_c}\sum_i n_i e^{i\mathbf{k}\cdot\mathbf{r}_i}, \tag{2}$$

where i labels individual vortices, and n_i and $\mathbf{r}_i$ are the winding number and position of the ith vortex, while N_c is the total winding number. For a familiar crystal lattice, $|S(\mathbf{k})|$ displays peaks at the corresponding reciprocal lattice vectors. Here, we focus on following three cases: the triangular Abrikosov lattice in the absence of the OL (S_T) and the square (S_S) and the checkerboard (S_C) lattices defined by the OL. Each lattice structure has two fundamental reciprocal vectors. In this instance it is sufficient to calculate the structure factor along one dimension, i.e., for one of the reciprocal vectors. Our results are displayed in Fig. 2. We observe that as V_0 is increased from zero, the triangular lattice is destroyed over a very small range of V_0 as S_T exhibits a sudden jump, indicative of a first order transition which is physically expressed by the motion of vortices towards the pinning sites. When there are more vortices than pinning sites ($\eta > 1$), the surplus vortices get pinned at a comparatively ''slow'' pace as a consequence of repulsion experienced from vortices which are already pinned. Conversely, when the number of pinning sites exceeds that of vortices ($\eta < 1$), the fully pinned vortex lattice is quickly established.

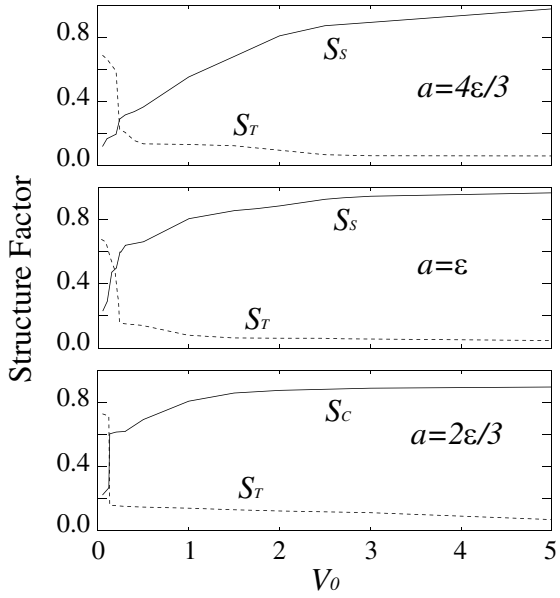

FIG. 2. Structure factors as functions of V_0 for $a = 4\epsilon/3$, ϵ, and $2\epsilon/3$. $S_{T,S,C} = |S(\mathbf{k}_{T,S,C})|$, where $\mathbf{k}_{T,S,C} = (2\pi/\epsilon)\hat{x} - [2\pi/(\sqrt{3}\epsilon)]\hat{y}$, $2k\hat{y}$ and $k\hat{x} - k\hat{y}$, representing, respectively, one of the two fundamental reciprocal vectors for the triangular, square, and checkerboard lattices.

We now turn to explore the structure of the fully pinned vortex lattice for various values of η. In the case where η is not close to an integer or inverse integer value, we observe the coexistence of sublattices of different geometry bounded by domain walls which always lie along the diagonal of the OL. For $\eta = 1.8$ we have the coexistence of two sublattices formed by doubly and singly quantized vortices, respectively [see Fig. 3(a)]. For this fully pinned vortex lattice, the domains have striped parallel walls (represented by the solid lines in the figure), indicating interdomain repulsion [17,18]. This can be understood as a consequence of the repulsive vortex-vortex interaction. For the slightly smaller value of $\eta = 1.6$, these two sublattices form two interlocking checkerboard structures [see Fig. 3(b)]. As a decreases further to 0.95ϵ [Fig. 3(c)], all doubly quantized vortices have disappeared and the vortex lattice becomes completely commensurate with the OL, with each pinning site hosting a singly quantized vortex. This represents the fully matching case of $\eta = 1$. Upon further decrease of a or η, Figs. 3(d) and 3(e) show that more pinning sites become unoccupied and the checkerboard domain begins to cover the whole lattice. In this ground state, the walls between the square and checkerboard domains are crossing each other, signifying an attractive domain wall interaction which may be intuitively understood as resulting from the tendency of the vortices to occupy the vacant pinning sites.

In the study of domain wall formation, we see again distinct advantages of BEC vortex lattices over alternative

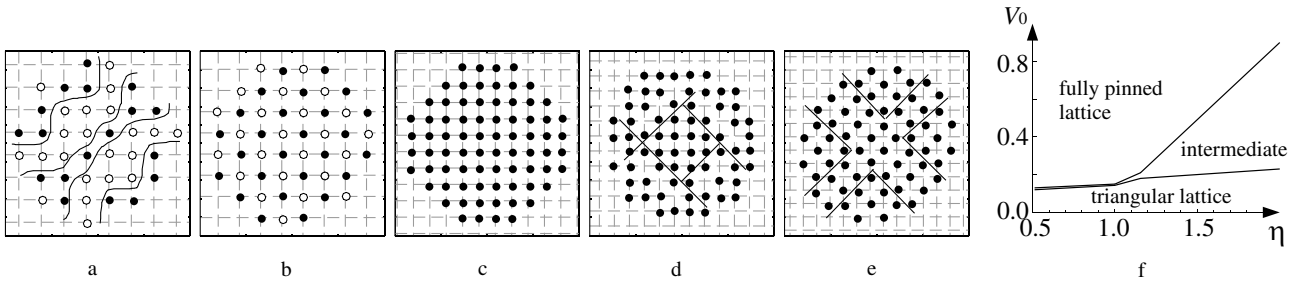

FIG. 3. (a)–(e) Structures of the fully pinned vortex lattice. From left to right, $\eta = 1.8, 1.6, 1.0, 0.8$, and 0.6, respectively. Solid lines represent domain walls. (f) Phase diagram of the pinned vortex lattice.

systems. Although similar domain formation was observed earlier in superconducting systems [10,19], their origin could not be clearly established because of additional defects likely to be present in the experimental samples. By contrast, in the atomic BEC system, the OL provides us with a defect-free periodic pinning potential and thus frees us to confidently investigate the more fundamental factors controlling the dynamics of domain formation and hence the structure of the domain walls. Recent success at directly imaging [2] and calculating [15] vortex-lattice excitations in BECs presents very exciting possibilities for studying, in unprecedented detail, the dynamics of the pinned vortex lattices obtained in this work and opens the door to more ambitious studies of structural phase transitions in unconventional geometries. Finally, we present in Fig. 3(f) a vortex-lattice phase diagram based on the structure factors. We call the lattice structure ''triangular lattice'' if $S_T > 0.5$, and ''fully pinned lattice'' if $S_S > 0.5$. Otherwise, it is termed as ''intermediate.'' For $\eta < 1$, there is a very small intermediate regime which quickly grows as η exceeds unity.

In summary, we have theoretically investigated the vortex state of a rapidly rotating condensate in a periodic optical potential. We have found that the vortex lattice exhibits a rich variety of structures depending on the parameters of the optical potential. In the future it will be interesting to investigate the detailed dynamics (e.g., time evolution) of the phase transitions between various structures and to relate the transitions to the properties of the condensate such as its collective excitation modes. Such studies will certainly shed new light on many other systems displaying structural phase transitions. Another problem to study concerns the situation when the OL becomes so strong that the condensate reaches the Mott insulator regime, as discussed recently by Wu *et al.* [20].

This work is supported by the NSF, the ONR, and the University of Rochester (L. O. B. and N. P. B.) and by Rice University (H. P. and S. Y.). L. O. B. is supported by the Laboratory for Laser Energetics Horton Program. N. P. B. is also with the Institute of Optics. We thank Ennio Arimondo for fruitful discussions.

Note added.—During the preparation of the Letter, we noticed the work of Reijnders and Duine [21] who studied some aspects of this system using a variational approach.

[1] *Structural Phase Transitions I and II*, edited by K. A. Müller and H. Thomas (Springer-Verlag, Berlin, 1981).
[2] I. Coddington *et al.*, Phys. Rev. Lett. **91**, 100402 (2003); V. Schweikhard *et al.*, Phys. Rev. Lett. **92**, 040404 (2004).
[3] D. Boiron *et al.*, Phys. Rev. A **57**, R4106 (1998); R. Dumke *et al.*, Phys. Rev. Lett. **89**, 097903 (2002); R. Newell *et al.*, Opt. Lett. **28**, 1266 (2003).
[4] Z. Chen and K. McCarthy, Opt. Lett. **27**, 2019 (2002).
[5] M. Greiner *et al.*, Nature (London) **415**, 39 (2002).
[6] D. Jaksch *et al.*, Phys. Rev. Lett. **81**, 3108 (1998).
[7] M. P. A. Fisher *et al.*, Phys. Rev. B **40**, 546 (1989).
[8] K. Harada *et al.*, Science **274**, 1167 (1996); S. B. Field *et al.*, Phys. Rev. Lett. **88**, 067003 (2002); W. V. Pogosov, A. L. Rakhmanov, and V. V. Moshchalkov, Phys. Rev. B **67**, 014532 (2003).
[9] C. Reichhardt, C. J. Olson, and F. Nori, Phys. Rev. B **57**, 7937 (1998); C. Reichhardt and N. Grønbech-Jensen, Phys. Rev. B **63**, 054510 (2001); C. Reichhardt *et al.*, Phys. Rev. B **64**, 144509 (2001).
[10] A. N. Grigorenko *et al.*, Phys. Rev. B **63**, 052504 (2001).
[11] U. R. Fischer and G. Baym, Phys. Rev. Lett. **90**, 140402 (2003).
[12] A. L. Fetter and A. A. Svidzinsky, J. Phys. Condens. Matter **13**, R135 (2001).
[13] Z. Tešanović and L. Xing, Phys. Rev. Lett. **67**, 2729 (1991).
[14] K. W. Madison *et al.*, Phys. Rev. Lett. **84**, 806 (2000); J. R. Abo-Shaeer *et al.*, Science **292**, 476 (2001); P. C. Haljan *et al.*, Phys. Rev. Lett. **87**, 210403 (2001); E. Hodby *et al.*, Phys. Rev. Lett. **88**, 010405 (2002).
[15] J. R. Anglin and M. Crescimanno, cond-mat/0210063; G. Baym, Phys. Rev. Lett. **91**, 110402 (2003); L. O. Baksmaty *et al.*, Phys. Rev. Lett. **92**, 160405 (2004); T. Mizushima *et al.*, Phys. Rev. Lett. **92**, 060407 (2004).
[16] Y. Shin *et al.*, Phys. Rev. Lett. **93**, 160406 (2004).
[17] P. Bak *et al.*, Phys. Rev. B **19**, 1610 (1979).
[18] K. Kern and G. Comsa, in *Chemistry and Physics of Solid Surfaces VII*, edited by R. Vanselow and R. Howe (Springer, Berlin, 1988).
[19] S. B. Field *et al.*, Phys. Rev. Lett. **88**, 067003 (2002).
[20] C. Wu *et al.*, Phys. Rev. A **69**, 043609 (2004).
[21] J. W. Reijnders and R. A. Duine, Phys. Rev. Lett. **93**, 060401 (2004).